PHYSICAL REVIEW B VOLUME 62, NUMBER 12 15 SEPTEMBER 2000-II

Magnetotunneling spectroscopic probe of quantization due to inhomogeneous strain in a Si/SiGe vertical quantum dot

Jun Liu,[1] A. Zaslavsky,[2] C. D. Akyüz,[1] B. R. Perkins,[2] and L. B. Freund[2]
[1]*Department of Physics, Brown University, Providence, Rhode Island 02912*
[2]*Division of Engineering, Brown University, Providence, Rhode Island 02912*
(Received 21 June 2000)

A columnar *p*-Si/SiGe quantum dot is etched from a strained layer structure. The creation of the stress-free lateral face of the column results in a spatially inhomogeneous strain field within the dot which can induce lateral quantum confinement, in addition to the usual vertical confinement. As a result, a fine structure appears in the resonant tunneling current-voltage $I(V)$ characteristics. Here we present the magnetotunneling $I(V,B)$ characteristics in parallel magnetic field $B \| I$ which provide an experimental probe of the hole states confined by the radially symmetric strain-induced potential in the quantum dot. The evolution of the fine structure with B reveals the influence of the magnetic confinement on the resulting one-dimensional ringlike hole subbands, which is consistent with numerical analysis of hole states of the quantum dot in magnetic field.

In the past decades rapid progress in epitaxial technology has made possible high-quality resonant tunneling devices in numerous semiconductor heterostructures.[1,2] Advances in fabrication technology make it possible to fabricate submicron-scale resonant tunneling (RT) diodes in which lateral confinement of the tunneling electrons is imposed so as to induce additional lateral quantization first observed in III-V quantum dots.[3–5] Si/SiGe double-barrier RT devices have drawn attention due to their potential compatibility with Si technology as well as new effects arising from strain.

Lattice mismatch between Si and SiGe introduces biaxial strain in the epitaxial layer, which remains homogeneous as long as the strained layer thickness stays below a certain critical thickness h_c.[6] The strain lifts the degeneracy of the heavy-hole (HH) and light-hole (LH) valence-band edges and reshapes the HH and LH dispersions. When a quantum dot is etched out of the strained heterostructure, the biaxial strain can relax as demonstrated by Raman spectroscopy[7] and resonant tunneling measurements.[8,9] Recently, experiments have confirmed that the strain relaxation in the quantum dot is inhomogeneous, which induces additional lateral confinement of holes in the quantum well.[8–10] We have utilized RT measurement to probe the inhomogeneous strain in an individual $Si/Si_{0.8}Ge_{0.2}$ double-barrier quantum dot. The fine structure in the HH $I(V)$ characteristics reveals the discrete hole states confined by the in-plane ringlike potential associated with an axially symmetric strain distribution in the quantum well. The evolution of the fine structure with magnetic field shows the competition between the magnetic confinement and the inhomogeneous-strain-induced lateral potential, which is consistent with our numerical analysis of the density of states of the quantum dot in various magnetic fields. The analysis incorporates a nonuniform strain profile in the partially relaxed quantum dot determined by the finite element method.

The vertical quantum dot we measured was fabricated from strained *p*-Si/SiGe double-barrier resonant tunneling material. The nominally undoped double-barrier region consists of a strained 35-Å $Si_{0.8}Ge_{0.2}$ quantum well confined by two 45-Å Si barriers. There are 200-Å undoped $Si_{0.8}Ge_{0.2}$ spacer layers graded to p^+-Si contact regions on either side of the active region. Electron-beam lithography was used to define the quantum dot and reactive ion etching was utilized to acquire a deep submicron pillar of nominal diameter $D = 0.15$ μm (see Ref. 10). The applied bias between the top contact and the substrate aligns the hole states in the emitter electrode with the quantized hole states in the Si/SiGe quantum well, leading to resonant $I(V)$ peaks.[2,8] The heavy-hole and light-hole branches of the hole dispersion give rise to separate two-dimensional (2D) subbands and hence $I(V)$ peaks. In this paper we will focus on the HH $I(V)$ peak, because the HH states have a lighter in-plane mass[11] and hence are more sensitive to inhomogeneous-strain-induced lateral potentials we are interested in.

The HH peak in the $I(V)$ curve of the vertical quantum dot measured at $T = 1.7$ K along with that of a large $D = 2$ μm device are shown in Fig. 1. The shift of the HH peak of the smaller device towards higher bias is due to average strain relaxation, as reported previously.[8–10] We can estimate the average strain relaxation in our device by means of deformation potential theory[12] combined with a self-consistent calculation of the potential distribution over the active region.[8,10] The observed shift in bias of about 100 mV corresponds to $\sim$15 meV increase in the energy of the HH subband with respect to the Fermi sea in the emitter. This change of subband energy can be converted into $\sim$70% relaxation of the original strain energy by using deformation potential theory and 6×6 Luttinger-Kohn Hamiltonian.[11–13] These estimations are consistent with our finite element calculations as shown in Fig. 2.

In addition to the overall shift due to average strain relaxation, there exist several small peaks superimposed on the HH resonant peak of the $D = 0.15$ μm device while the reference line shape of the $D = 2$ μm device is quite smooth without any fine structure. The fine structure appears in both polarities of bias and is reproducible upon temperature cycling. The separation of the positions of the small peaks range from 10 to 30 mV, which are corresponding to quan-

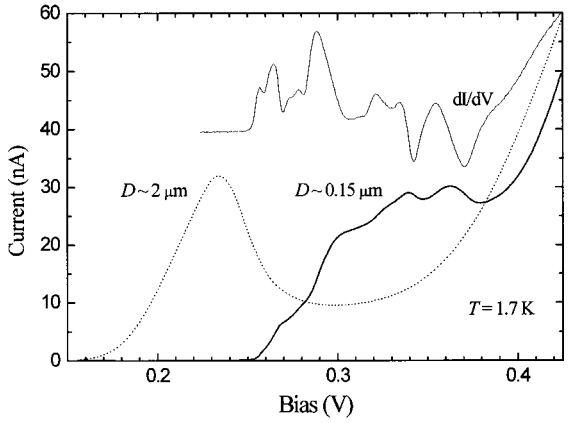

FIG. 1. HH resonant tunneling $I(V)$ and dI/dV characteristics at $T=1.7$ K of a $D=0.15$ μm vertical quantum dot made of p-Si/$Si_{0.8}Ge_{0.2}$ double-barrier material, showing strong fine structure. The dashed line shows the smooth HH $I(V)$ characteristic of a $D=2$ μm quantum dot for comparison.

tized hole energy difference ranging from 2 to 7 meV. The geometric lateral quantization energy $\sim\hbar^2/2m^*D^2$ and the single electron charging energy $\sim e^2/C$ (where C is the dot capacitance to the ground) are too small to account for these peaks. The magnitude of the small peaks and the fact that similar fine structure has been observed in other submicron quantum dots made of similar materials exclude the possibility of tunneling via impurities in the quantum well.[10] Furthermore, unlike the HH peak, the LH resonant peak (not shown) does not show any fine structure, apart from the shift of peak position arising from average strain relaxation.[8] Fine structure in the LH peak has been observed in a smaller quantum dot $D=0.1$ μm,[10] where the strain profile was even more inhomogeneous.

We attribute the fine structure to the tunneling into the discrete hole states confined by the in-plane inhomogeneous-strain-induced potential in the quantum well. Finite element simulations based on a linear elastic model are employed to calculate the strain components of cylindrical Si/$Si_{0.8}Ge_{0.2}$ double-barrier pillars of various diameters D.[12] The results are shown in Fig. 2. The calculated radial strain component ε_{rr} is plotted as a function of in-plane radius $r_\perp$ for the $D=0.1-0.2$ μm range in Fig. 2 (top curves). As shown in Fig. 2, the average strain relaxation becomes larger while the strain profile becomes more inhomogeneous as the size of the quantum dot decreases. For $D=0.15$ μm device, ε_{rr} decreases gradually with $r_\perp$ except for a region of increasing strain near the surface. The resulting ringlike large strain regions exceeds ~100 Å with relative $\varepsilon_{rr}\sim 0.6$ whereas the relative ε_{rr} is only about 0.3 in the center of the pillar.

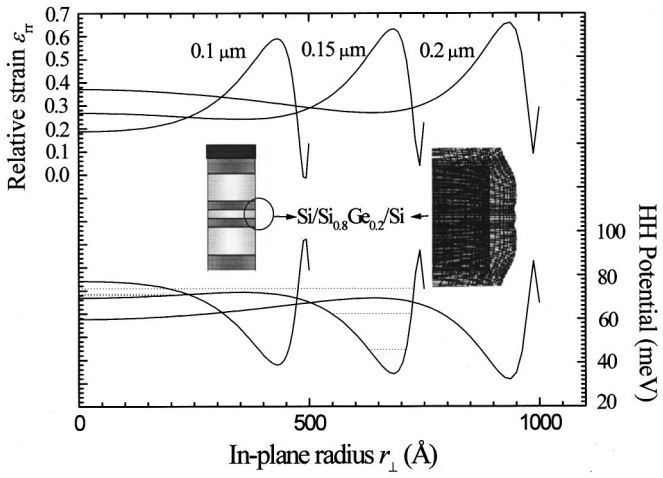

FIG. 2. The top curves show the calculated radial strain component ε_{rr} ($r_\perp$) for $D=0.1$, 0.15, and 0.2 μm devices on the midplane of the $Si_{0.8}Ge_{0.2}$ quantum well (full biaxial strain corresponds to $\varepsilon_{rr}=1$). The inset shows the magnified view of the finite element mesh for the active region near the sidewall. The bottom curves are the corresponding inhomogeneous-strain-induced in-plane confining potentials for HH as a function of $r_\perp$ in the well. The dashed lines mark the confined ringlike subbands in the $D=0.15$ μm device we studied.

Since the strain in the strained SiGe layer determines the electronic properties of the material, radially inhomogeneous strain induces a lateral potential for the holes in the well. We use six-band Luttinger-Kohn Hamiltonian to calculate the HH subband energy at $k_\perp=0$ as a function of local strain which is a function of in-plane radius $r_\perp$. The lower three curves in Fig. 2 are the resulting lateral potentials for the heavy holes in the $Si_{0.8}Ge_{0.2}$ quantum well. The larger strain in the ringlike region near the perimeter gives rise to a ringlike confining potential for the heavy holes, which can accommodate several ringlike bound states of HH. For devices with $D=0.2$ μm, the heavy holes can be quantized both by the ringlike potential and the central roughly parabolic potential, whereas for device with $D=0.1$ μm, the ringlike potential dominates. Analogous inhomogeneous potentials also appear in the emitter, but there they are screened by the large density of holes. Accordingly, the observed fine structure is mainly the consequence of tunneling of emitter holes into the laterally confined hole states in the quantum well. A full-scale calculation of the hole states in such quantum dots is extremely complicated, but treating HH as particles of constant mass $m^*=0.3m_e$,[14] we obtain several quantized states and 1D subbands in both the center region and the ringlike region at the perimeter, as shown in Fig. 2.

In order to investigate the hole states in the quantum dot, we have measured the $I(V)$ characteristics in different magnetic fields parallel to the tunneling direction $B\|I$. The results are shown in Fig. 3, including both bias polarities. Although the double-barrier heterostructure is nominally symmetric, dopant migration during the growth introduces asymmetries in the $I(V)$ characteristics. The fine structure is sharper in reverse bias because the onset of the rising background due to the tunneling through the higher-lying LH subband occurs at a higher voltage. The numbers and the positions of the small peaks and the line shapes of $I(V)$ curves in both polarities are similar. Also shown in Fig. 3 is the evolution of fine structure in an increasing B field. The positions have been converted to the relative bias (alignment) between the emitter and the well by self-consistent calculation, with respect to the threshold V_T where the current starts to flow (see Fig. 3). Interestingly, some of the peaks shift to lower bias as B field is increased, contrary to our intuition that B field should increase the energy of the quantized states. At a field around $B=5$ T, some peaks split into two.

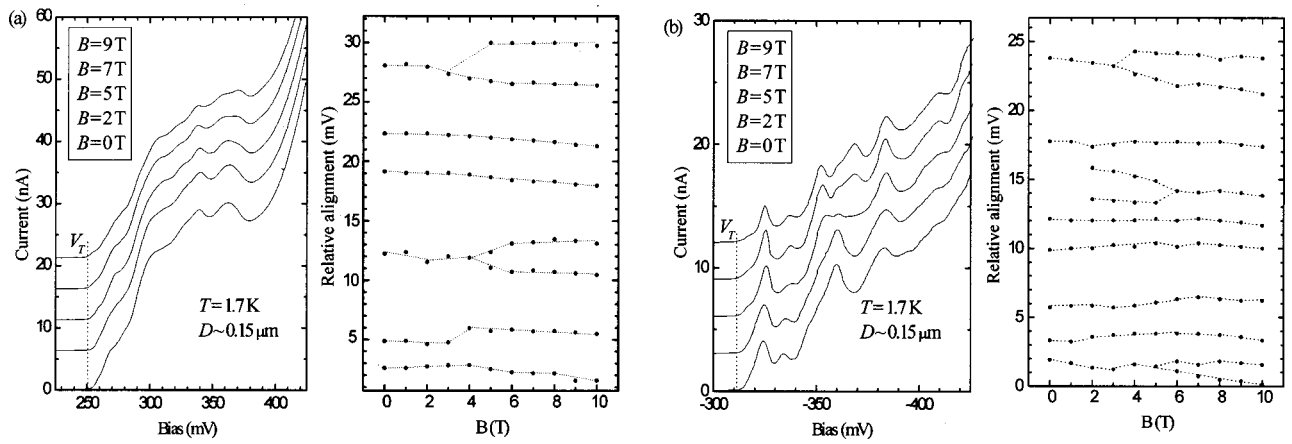

FIG. 3. (a) Heavy-hole $I(V,B)$ curves of the $D=0.15$ μm device at various B in forward bias at $T=1.7$ K. The relative bias (alignment) between the emitter and the well corresponding to each small peak superimposed on the main HH peak, with respect to the threshold V_T where current starts to flow, is plotted as a function of magnetic field. (b) Same data in reverse bias.

In the magnetic field, the holes are confined by both the lateral inhomogeneous-strain-induced potential and the magnetic field. We expect the evolution of small peaks with magnetic field to be the consequence of the competition between these two confinements. To simplify matters, we consider HH states to see the inhomogeneous-strain-induced confining potential in the quantum well as shown in the lower part of Fig. 2. The in-plane effective mass of heavy holes is taken to be constant at $0.3m_e$,[14] irrespective of the in-plane $k_\perp$. We calculated the density of states for a quantum dot of diameter $D=0.15$ μm in different magnetic fields by a numerical method, based on direct discretization of the Schrödinger equation. In the calculations, we assumed the Gaussian broadening of the individual states on the order of 1 meV, to account for finite temperature and scattering-limited lifetime effects. The results are shown in Fig. 4 with the lowest curve plots the density of the states at $B=0$. We can easily discern the three subbands arising from the quantization of the ringlike potential at the perimeter together with weaker quantization from the central parabolic region.

Now consider the situation in which the B field is turned on. In symmetric gauge, the 2D Landau levels in free space are given by

$$\varepsilon_{nl}=(n-\tfrac{1}{2}l+\tfrac{1}{2}|l|-\tfrac{1}{2})\hbar\omega_c, \qquad (1)$$

where l is the angular momentum quantum number, and ω_c is the cyclotron frequency. The eigenstates occupy annular regions that are located farther from the center if l is larger. We notice that ε_{nl} is independent of l for $l>0$. The decreasing magnetization energy compensates the increase of energy due to the increase of angular momentum. In our case, instead of free space, the holes are also confined by the inhomogeneous-strain-induced lateral potential. When the annular region is located in the ringlike well where the lateral potential is the lowest, we expect the state to have the lowest energy. This is confirmed by our numerical calculations of the energy states in the inhomogeneous-strain-induced potential and external magnetic field. In magnetic field the ground state has a large angular momentum. On the other hand, a simple model of a circular one-dimensional wire also indicates the same behavior of eigenstates in magnetic field.[15] As the magnetic field increases, the ground state of the 1D wire will have higher and higher positive angular momentum quantum number. Experiments have confirmed this observation in self-assembled quantum rings.[16] Consequently, the lowest energy level for each subband is shifting to higher angular momentum as the magnetic field is increased. In the emitter, on the other hand, the strain-induced lateral potential is weaker and is also screened by the large hole density. As a result, the energy of the emitter Landau levels remains relatively insensitive to l. Since tunneling into the well conserves l as a result of the cylindrical symmetry,[17] the RT peaks due to tunneling into the 1D ringlike subbands can be expected to shift to lower bias. Our numerical calculations show that the density of states of the lower two 1D ringlike subbands do not change significantly with the magnetic field up to 10 T, though the angular momentum shifts to higher value. The third subband, which corresponds to the shallowly bound states near the top of the ringlike potential well, splits into two smaller bands at $B\sim5$ T. The splitting is the consequence of the interaction between the ringlike confinement and the central parabolic potential within the perpendicular magnetic field. The magnetic length at 5 T, which

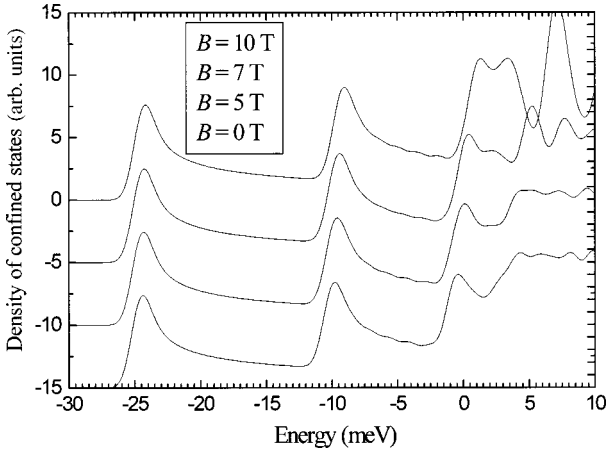

FIG. 4. Density of laterally quantized states of a $D=0.15$ μm quantum dot in different magnetic fields, calculated by numerical method using the lateral inhomogeneous-strain-induced potential shown in Fig. 3. The calculations assume ~1 meV broadening of individual hole states.

is around 150 Å, is comparable with the width of the top of the ringlike well. Thus, our very simple model is in good qualitative agreement with the experiment, but we stress that a more thorough analysis, including the complexities of the valence band dispersion, is needed for a true quantitative model.

In conclusion, magnetotunneling is utilized to probe the effects of inhomogeneous strain and associated hole states in an isolated vertical p-$Si/Si_{0.8}Ge_{0.2}$ double-barrier resonant-tunneling structure of diameter ~ 0.15 μm. Several small peaks superimposed on the dominant HH peak were observed. We attribute the fine structure to the tunneling into the ringlike hole subbands quantized by the in-plane ringlike confining potential arising from inhomogeneous strain in the quantum well. The experimental observations are consistent with our finite element calculation of the strain profile and numerical calculations of the density of states based in the inhomogeneous-strain-induced potential. Ringlike structures have been investigated by various methods such as millimeter-wave spectroscopy,[18] and far-infrared transmission spectroscopy,[16] usually performed on large numbers of devices simultaneously, as well as Ahronov-Bohm conductance measurement.[19] The inhomogeneous strain relaxation in the quantum dot provides another way to make a single mesoscopic ring structure, and tunneling spectroscopy can be utilized to probe the resultant 1D ringlike subbands. The above studies also show that the inhomogeneous strain relaxation in strained structures can induce large variations in their electronic properties.

The authors thank Brad Marston for insightful discussions. The work at Brown was supported by the NSF (Grant No. DMR-9702725) and the NSF MRSEC Center (Grant No. DMR-9632524). The fabrication facilities were also supported in part by Brown MRSEC.

[1] L. L. Chang, L. Esaki, and R. Tsu, Appl. Phys. Lett. **24**, 593 (1974).
[2] H. C. Liu, D. Landheer, M. Buchanan, and D. C. Houghton, Appl. Phys. Lett. **52**, 1809 (1988).
[3] M. A. Reed, J. N. Randall, R. J. Aggarwal, R. J. Matyi, T. M. Moore, and A. E. Wetsel, Phys. Rev. Lett. **60**, 535 (1988).
[4] Bo Su, V. J. Goldman, and J. E. Cunningham, Phys. Rev. B **46**, 7644 (1992).
[5] S. Tarucha, D. G. Austing, Y. Tokura, W. G. van der Wiel, and L. P. Kouwenhoven, Phys. Rev. Lett. **84**, 2485 (2000).
[6] J. C. Bean, L. C. Feldman, A. T. Fiory, S. Nakahara, and I. K. Robinson, J. Vac. Sci. Technol. A **2**, 436 (1984).
[7] A. A. Darhuber, T. Grill, J. Stangl, and G. Bauer, Phys. Rev. B **58**, 4825 (1998).
[8] A. Zaslavsky, K. R. Milkove, Y. H. Lee, B. Ferland, and T. O. Sedgwick, Appl. Phys. Lett. **67**, 3921 (1995).
[9] P. W. Lukey, J. Caro, T. Zijlstra, E. Van der Drift, and S. Radelaar, Phys. Rev. B **57**, 7132 (1998).
[10] C. D. Akyüz, A. Zaslavsky, L. B. Freund, D. A. Syphers, and T. O. Sedgwick, Appl. Phys. Lett. **72**, 1739 (1998).
[11] J. M. Luttinger, Phys. Rev. **102**, 1030 (1956).
[12] H. T. Johnson, L. B. Freund, C. D. Akyüz, and A. Zaslavsky, J. Appl. Phys. **84**, 3714 (1998).
[13] C. D. Akyüz, Ph.D. thesis, Brown University, 1999 (unpublished).
[14] J. P. Cheng, V. P. Kesan, D. A. Grutzmacher, T. O. Sedgwick, and J. A. Ott, Appl. Phys. Lett. **62**, 1522 (1993).
[15] T. Chakraborty and P. Pietiläinen, Phys. Rev. B **50**, 8460 (1994).
[16] Axel Lorke, R. Johannes Luyken, Alexander O. Govorov, and Jörg P. Kotthaus, Phys. Rev. Lett. **84**, 2223 (2000).
[17] E. E. Mendez, L. Esaki, and W. I. Wang, Phys. Rev. B **33**, 2893 (1986).
[18] C. Dahl, J. P. Kotthaus, H. Nickel, and W. Schlapp, Phys. Rev. B **48**, 15 480 (1993).
[19] A. F. Morpurgo, J. P. Heida, T. M. Klapwijk, and B. J. van Wees, Phys. Rev. Lett. **80**, 1050 (1998).